

Flux dependence of carbon erosion and implication for ITER

J. Roth ^{a,*}, A. Kirschner ^b, W. Bohmeyer ^f, S. Brezinsek ^b, A. Cambe ^d,
E. Casarotto ^b, R. Doerner ^g, E. Gauthier ^d, G. Federici ^h, S. Higashijima ^e,
J. Hogan ^d, A. Kallenbach ^a, H. Kubo ^e, J.M. Layet ^d, T. Nakano ^e, V. Philipps ^b,
A. Pospieszczyk ^b, R. Preuss ^a, R. Pugno ^a, R. Ruggiéri ^d,
B. Schweer ^b, G. Sergienko ^b, M. Stamp ^c

^a Max-Planck-Institut für Plasmaphysik, EURATOM Association, Boltzmannstrasse 2, D-85748 Garching, Germany

^b Institut für Plasmaphysik, Forschungszentrum Jülich, EURATOM Association, D-52425 Jülich, Germany

^c EURATOM/UKAEA Fusion Association, Culham Science Center, Abingdon OX14 3DB, UK

^d Association EURATOM-CEA, CEA Cadarache, F-13108 St. Paul lez Durance, France

^e Japan Atomic Energy Research Institute, Naka-machi, Muka-gun, Ibaraki-ken 311-0193, Japan

^f Max-Planck-Institut für Plasmaphysik, EURATOM Association, Mohrenstr. 42, D-10117 Berlin, Germany

^g Fusion Energy Research Program, University of California San Diego, La Jolla, CA 92093-0417, USA

^h ITER JWS Garching Co-center, Boltzmannstr. 2, D-85748 Garching, Germany

Abstract

In a collaboration of eight experiments the dependence of the chemical erosion yield of carbon on the ion flux, Φ , was established to $\Phi^{-0.54}$ at high ion fluxes. With this flux dependence a comprehensive description for chemical erosion is available as function of energy, temperature and flux. With this description the erosion and re-deposition of carbon in the ITER divertor can be calculated using the ITER steady-state plasma scenario and the ERO code. The resulting gross and net erosion rates during steady-state phase of discharges are compared to previous estimates using a constant erosion yield of 1.5%. The use of the complete parameter dependence results in an order of magnitude lower erosion, and, accordingly, of the T codeposition inventory.

© 2004 Elsevier B.V. All rights reserved.

PACS: 28.52.Fa; 82.65.-i; 52.25.Fi; 52.40.Hf

Keywords: Tritium inventory; Co-deposition; Chemical erosion; ERO-code; ITER

1. Introduction

The erosion of plasma-facing materials in magnetically confined fusion devices is a key issue especially

regarding the tritium inventory [1]. Tritium retention is dominated by the inventory retained in deposited layers of eroded material, such that erosion is the starting point of processes leading to build-up of tritium.

Erosion due to energetic particle bombardment depends on a number of parameters such as particle energy and flux, as well as surface temperature and has seen a remarkable degree of clarification within the last decade [2–5]. Simultaneously, ion beam experiments at energies

* Corresponding author. Tel.: +49 89 3299 1387; fax: +49 89 3299 2279.

E-mail address: roth@ipp.mpg.de (J. Roth).

down to 10 eV [6,7] have improved the understanding of ion induced hydrocarbon emission as function of energy and temperature. A recent paper collects data from ion beams, plasma simulators, and fusion devices, covering 4 orders of magnitude in flux and resulting in a reliable formulation of the flux dependence [8].

The addition of the flux dependence results in a complete description of chemical erosion as function of energy, surface temperature and particle flux. This complete description will make more precise erosion and re-deposition estimates possible than previous conservative assumptions using a constant chemical erosion yield of 1.5%.

2. Flux dependence of chemical erosion

The investigation of chemical erosion has been performed for thermal hydrogen atom or ion fluxes of the order of 10^{16} – $10^{20}/\text{m}^2\text{s}$. The model predicts a pronounced shift of the temperature maximum, T_{max} , towards higher temperatures with increasing flux. This temperature shift is well reproduced in experimental data [9]. However, at fluxes above $10^{21}/\text{m}^2\text{s}$ as reached under tokamak conditions, T_{max} reaches values where the annealing of radiation damage results in a reduced reactivity of the carbon material. This has led to the prediction that at such high fluxes the yield at T_{max} decreases.

Today, measured yield data are available from the plasma simulators PSI-1 [10] and PSI-2 [11], PISCES-B [12], and from plasma edge and divertor measurements in the fusion facilities JET [13], Tore Supra [14,15], TEXTOR [16], ASDEX Upgrade [17], and JT-60 U [18]. With the exception of JT-60U, where the calibration of the spectroscopic parameters for the CD- and C_2 -bands were taken from PISCES [19], in all other devices the signals were calibrated by in situ hydrocarbon gas puffs.

After re-evaluation and normalisation of the data, a set of high flux data for methane production is available (Fig. 1) [8]. The data are for D^+ , normalised to an incident ion energy of 30 eV and selected to be taken at or near T_{max} . Three individual data sets performed in a narrow flux range could not distinguish a clear flux dependence (PISCES, JET, JT-60U) as stated by the authors [12,13,18]. However, the ensemble of data points and the investigations of PSI-1, TEXTOR and Tore Supra, spanning flux ranges of more than an order of magnitude, suggest a decrease of the erosion yield with ion flux, Φ , starting at fluxes of about $10^{21}/\text{m}^2\text{s}$.

As all investigators have provided error bars for their yield values, a fit to the data using Bayesian probability theory was made taking these errors into account [20]. This resulted in a decrease of the yield at high fluxes according to

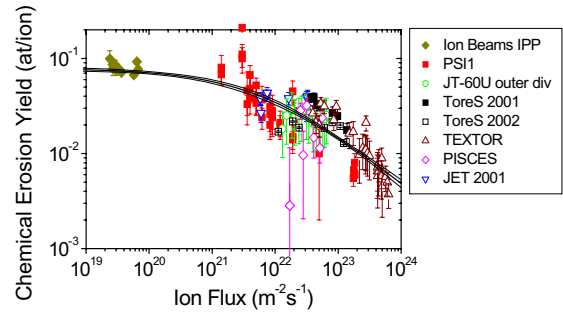


Fig. 1. Flux dependence of the chemical erosion yield for T_{max} and 30 eV D^+ determined from different plasma experiments [8]. The thin lines indicate the confidence interval of the data.

$$Y(E, T, \Phi) = \frac{Y_{\text{low}}(E, T)}{1 + \left(\frac{\Phi}{6 \times 10^{21}}\right)^{0.54}} \quad (1)$$

The exponent at high ion fluxes was determined to 0.54 ± 0.04 . The same flux dependence, as given for T_{max} seems also to apply at room temperature (see results from ASDEX Upgrade [17]). Therefore, it can be assumed that at all temperatures the same factor applies to the analytical description of chemical erosion, $Y_{\text{low}}(E, T)$, given previously [5]. A description is now available which covers the energy, temperature and flux dependence adequately for extrapolation to wall and divertor conditions in ITER. There remain still uncertainties concerning the contribution of heavier hydrocarbons to the total erosion yield. In [5] an additional factor of 1.3 takes account of heavier hydrocarbons, but this factor needs further investigations, especially at low ion energies.

3. Implications for carbon erosion and re-deposition in ITER

3.1. ITER conditions

In ITER carbon material will only be used for the strike-point tiles in the divertor. Previous divertor erosion and re-deposition evaluations use a semi-detached plasma scenario [21]. The same plasma scenario is now used for improved erosion and re-deposition estimation during steady-state phase of discharges. Fig. 2 shows the plasma electron and ion temperature, and density as well as power load and surface temperature across the divertor plate of the outer ITER divertor. Note that the plasma scenario represents ELM free conditions and the additional effect of ELM erosion [22] has to be evaluated separately.

The surface temperature was estimated for a CFC material with reduced thermal conductivity due to n-irradiation [23]. For these extreme conditions the

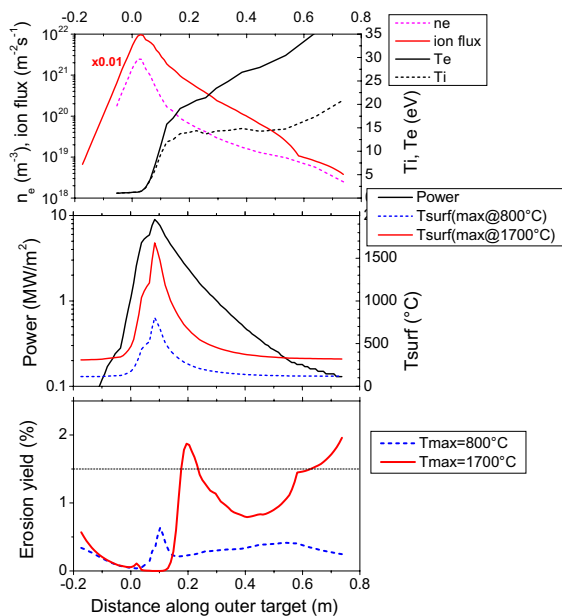


Fig. 2. Divertor plasma and tile surface conditions and erosion yields in the outer ITER divertor [21]. Temperatures were calculated for standard operation (max@800°C) and for thick, n-damaged CFC tiles (max@1700°C) [23].

temperature in the outer divertor reaches 1700°C, where chemical erosion can be neglected. Thermal and radiation enhanced sublimation (RES) of carbon is not yet of importance even at the peak temperatures [24] under high flux conditions. In the initial phase of ITER no n-damage effects are expected. Therefore, average operation conditions with higher thermal conductivity and thinner carbon tiles resulting in maximum temperatures of 800°C for the outer divertor [25] are included in the analysis.

Beryllium originating from the main wall will be transported preferentially into the inner divertor and reduce chemical erosion due to surface coverage [26]. Therefore, estimation of the erosion for the inner divertor is much more uncertain. Erosion simulations will be presented neglecting the reduction of carbon erosion due to beryllium coverage and assuming average operation conditions leading to a maximum surface temperature of about 300°C.

3.2. Gross erosion estimates

In previous estimates no flux dependence of the erosion yield has been assumed and the yield was taken independent of ion energy and temperature at a constant value of 1.5% [27]. The eroded atoms were followed using the REDEP code until final deposition. In the present evaluation of erosion, transport and re-deposi-

tion the Monte-Carlo code ERO was used in the ITER divertor geometry [28]. Erosion processes such as physical and chemical sputtering are incorporated in the code, using for comparison a fixed yield of 1.5% or the full description as function of energy, surface temperature and particle flux. Eroded atoms and molecules (CH₄ and higher hydrocarbons) are followed through ionisation, dissociation, excitation until they are re-deposited at the divertor plates or leave the user-defined simulation volume. Local particle transport includes friction, thermal and Lorentz forces. For dissociation and ionisation of hydrocarbon molecules the data set from Janev [29] is used.

Fig. 2 includes the erosion yield for the two temperature conditions. In the case of $T_{\max} = 1700^\circ\text{C}$ chemical erosion is negligible at the strike point, but reaches values higher than 1.5% in the wings of the temperature distribution, where the fluxes are low and ion energies increase. For $T_{\max} = 800^\circ\text{C}$ the maximum chemical erosion occurs at the strike point, due to the high particle flux the value reaches only 0.5%.

Gross erosion values are given in Table 1 for all conditions assumed presently. For cases where chemical erosion is the dominant erosion process, the gross erosion values are more than an order of magnitude lower using the full description of chemical erosion compared to a fixed yield of 1.5%. Chemical erosion is reduced about to the level of physical sputtering in the outer divertor. In the inner divertor, the low surface temperatures lead to a drastic reduction of chemical erosion, while the low ion energies strongly reduce physical sputtering.

3.3. Re-deposition and net erosion

Carbon atoms returning to the divertor target will reduce gross erosion due to re-deposition. The effect of re-deposition depends strongly on the reflection coefficient for carbon atoms or the sticking coefficient S for hydrocarbon radicals. The reflection coefficients for carbon atoms are taken from MolDyn calculations [30], in general around 0.3 for the given plasma conditions. For hydrocarbon radicals S is varied between 0 and 1 [31], and assumed to be zero for fully saturated hydrocarbon molecules. While sticking coefficients of 1 for radicals are included to indicate the upper limit of re-deposition, such values are not considered reasonable [32]. On the contrary, sticking coefficients of zero had to be assumed in recent evaluations of the deposition pattern after ¹³CH₄ gas-puff experiments at the TEXTOR test limiter and of the erosion in the JET divertor [31]. The low 'effective' sticking coefficients include the effect of synergistic re-erosion by hydrogen atoms carried in the molecule and simultaneously incident energetic ions. Such low sticking coefficients only apply to surfaces with direct plasma contact.

Table 1

Gross erosion fluxes per 1 m of toroidal divertor length and re-deposition fractions calculated for two different assumptions on chemical erosion yield and sticking coefficients

		Full description		Fixed (1.5%)	
		S = 1	S = 0	S = 1	S = 0
<i>Outer divertor target</i>					
$T_{\max} = 1700^{\circ}\text{C}$	Gross erosion ($\text{m}^{-1}\text{s}^{-1}$)		2.6×10^{20}		3.4×10^{21}
	Re-deposition	99.6%	93.1%		
$T_{\max} = 800^{\circ}\text{C}$	Gross erosion ($\text{m}^{-1}\text{s}^{-1}$)		2.3×10^{20}		
	Re-deposition	99.6%	94.3%	99.5%	79.7%
Physical sputt.	Gross erosion ($\text{m}^{-1}\text{s}^{-1}$)		2.6×10^{20}		
	Re-deposition	97%			
<i>Inner divertor target</i>					
$T_{\max} = 300^{\circ}\text{C}$	Gross erosion ($\text{m}^{-1}\text{s}^{-1}$)		9.7×10^{19}		4.3×10^{21}
	Re-deposition	99.4%	86.6%	99.9%	76.6%
Physical sputt.	Gross erosion ($\text{m}^{-1}\text{s}^{-1}$)		8.5×10^{18}		
	Re-deposition	90%			

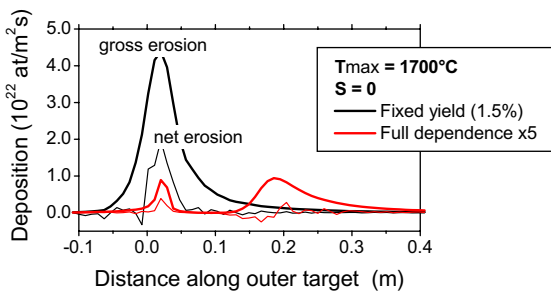


Fig. 3. Gross and net carbon erosion at the outer ITER divertor plate for fixed yield of 1.5% and with full yield dependence on energy, temperature and flux (multiplied by a factor of 5 for clarity).

In Fig. 3 an example is given for the gross and net erosion at the outer ITER divertor plate. Conditions are chosen for the extreme case of $T_{\max} = 1700^{\circ}\text{C}$ and all hydrocarbons returning to the surface have sticking coefficient $S = 0$. For a constant erosion yield of 1.5% the re-deposition on the target plate reduces the net erosion to 20% of the gross erosion. Taking the full energy, temperature and flux dependence into account the gross erosion amounts to only 7.6% of the erosion at fixed yield, the re-deposition on the target reaches 93% of the gross erosion. Similar reduction factors are found for other conditions, i.e. reduced temperatures at the outer divertor plate, and for the inner divertor at 300°C . Using the full description of chemical erosion reduces the gross erosion by a factor of about 30 compared to a fixed yield of 1.5%. The results for outer and inner divertor plate also including the effect of physical sputtering are summarised in Table 1, values for erosion and re-deposition rates are given for a toroidal divertor length of 1 m.

3.4. T inventory in carbon layers

For the analysis of the tritium inventory from co-deposition only the fraction of eroded atoms is taken into account which is not locally re-deposited on the divertor tiles. This fraction is transported to surfaces without plasma contact and builds up layers there. On surfaces without plasma contact, sticking coefficients of hydrocarbon radicals are found to be large [33] and will determine whether deposition occurs in direct line-of-sight to the divertor plates or in remote areas [34]. In previous estimations these re-deposited layers were assumed to contain a $(D + T)/C$ ratio of 0.4. This led to the conclusion that the in-vessel limit of 350 g tritium was reached after 70 to 180 ITER discharges within the error bars of the estimate [27,35].

For the present evaluation the same tritium concentration in the layers is assumed, although depending on surface temperature values between $T/C = 0.5$ (room temperature) or $T/C = 10^{-2}$ (high temperature) are found in present tokamak devices [33,36]. Fig. 4 gives

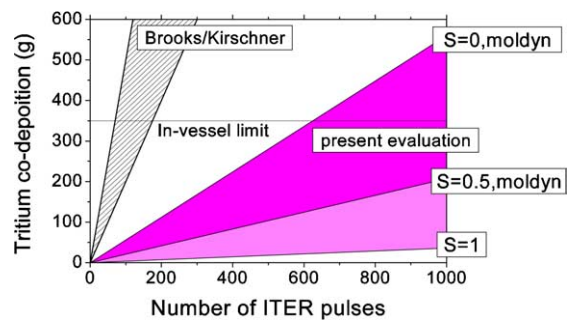


Fig. 4. T inventory vs ITER pulses evaluated using the full description of chemical erosion compared to previous estimates using a fixed erosion yield of 1.5%. Maximum surface temperature 800°C , no ELM erosion included.

the results of the expected T inventory as function of the number of full, 400s ITER discharges for the standard case of $T_{\max} = 800^\circ\text{C}$ compared to previous estimates [27,35]. Chemical and physical sputtering are considered, both from the outer and inner divertor targets. The use of the full description of the chemical sputtering yield extends the in-vessel limit to more than 600 steady-state discharges.

4. Conclusion

Important improvements in the consistency of data for the flux dependence of chemical erosion have been achieved by co-ordinated evaluation of data from ion beams, plasma simulators and fusion devices. This led to a clear flux dependence and a reduction of expected erosion yield at $10^{24}/\text{m}^2\text{s}$ from 3×10^{-2} to $\leq 5 \times 10^{-3}$. The use of an erosion yield dependent on energy, temperature and flux has improved the predictive capability compared to a constant erosion yield.

Using the full description of chemical erosion rather than a fixed yield independent of energy, temperature and flux reduces the gross erosion at the outer divertor by more than one order of magnitude and in the inner divertor by a factor of 30. The assessment of the fraction redeposited onto the divertor plates depends critically on the sticking coefficients for ions and hydrocarbon radicals. Assuming the minimum value of zero for all radicals, thus including synergistic re-erosion processes, still leads to a factor of about 5 less net erosion and T inventory per ITER discharge.

The present evaluations do not solve the problem of T inventory. Even for steady state plasmas, there still remains the task of regular removal of deposited carbon layers and recovery of the T content, although not at the previously predicted short intervals. In addition, erosion due to ELM sublimation will have to be investigated and taken into account.

Acknowledgment

This work was made possible by collaborations within the EU Task Force on PWI, Special Expert Group on Chemical Erosion, and ITPA, SOL and Divertor Physics.

References

- [1] G. Federici et al., Nucl. Fusion 41 (2001) 1967.
- [2] J. Roth, in: R.K. Janev, H.W. Drawin (Eds.), Atomic and Plasma-Material Interaction Processes in Controlled Thermonuclear Fusion, Elsevier, Amsterdam, 1993.
- [3] A. Horn, A. Schenk, J. Biener, B. Winter, C. Lutterloh, M. Wittmann, J. Küppers, Chem. Phys. Lett. 231 (1994) 193.
- [4] J. Roth, C. Garcia-Rosales, Nucl. Fusion 36 (1996) 1647, with corrigendum, Nucl. Fusion 37 (1997) 897.
- [5] J. Roth, J. Nucl. Mater. 266–269 (1999) 51.
- [6] B.V. Mech, A.A. Haasz, J.W. Davis, J. Appl. Phys. 84 (1998) 1655.
- [7] M. Balden, J. Roth, J. Nucl. Mater. 280 (2000) 39.
- [8] J. Roth et al., Nucl. Fusion 44 (2004) 21.
- [9] J. Roth, J. Bohdansky, K.L. Wilson, J. Nucl. Mater. 111&112 (1982) 775.
- [10] H. Grote et al., J. Nucl. Mater. 266–269 (1999) 1059.
- [11] P. Kornejew, W. Bohmeyer, H.-D. Reiner, C.H. Wu, Phys. Scr. T 91 (2001) 29.
- [12] D.G. Whyte, G.R. Tynan, R.P. Doerner, J.N. Brooks, Nucl. Fusion 41 (2001) 47.
- [13] M.F. Stamp, S.K. Erents, W. Fundamenski, G.F. Matthews, R.D. Monk, Phys. Scr. T 91 (2001) 13.
- [14] R. Ruggieri et al., J. Nucl. Mater. 266–269 (1999) 660.
- [15] A. Cambe, E. Gauthier, J. Hogan, J.M. Layet, J. Nucl. Mater. 313–316 (2003) 364.
- [16] A. Pospieszczyk, Phys. Scr. T 81 (1999) 48.
- [17] R. Pugno et al., J. Nucl. Mater., these Proceedings. doi:10.1016/j.jnucmat.2004.09.053.
- [18] T. Nakano et al., Nucl. Fusion 42 (2002) 689.
- [19] A. Pospieszczyk et al., UCLA-PPG-1251 (1989).
- [20] V. Dose, J. Roth, R. Preuss, J. Nucl. Mater. 288 (2001) 153.
- [21] G. Federici et al., J. Nucl. Mater. 313–316 (2003) 11.
- [22] G. Federici, A. Loarte, G. Strohmayer, Plasma Phys. Control. Fusion 45 (2003) 1523.
- [23] V. Barabash, G. Federici, J. Linke, C.H. Wu, J. Nucl. Mater. 313–316 (2003) 42.
- [24] V. Philipps et al., J. Nucl. Mater. 196–198 (1992) 1106.
- [25] G. Federici, ITER Team Garching (2004), private communication.
- [26] R. Doerner, M.J. Baldwin, K. Schmid, Phys. Scr. T 111 (2004) 75.
- [27] J. Brooks, A. Kirschner, J. Nucl. Mater. 313–316 (2003) 424.
- [28] A. Kirschner, V. Philipps, J. Winter, U. Kögler, Nucl. Fusion 40 (5) (2000) 989.
- [29] R.K. Janev, D. Reiter, Collisional Process of Hydrocarbon Species in Hydrogen Plasmas: I. The Methane Family, Jülich Report Jül-3966 (2002).
- [30] D. Rusic, D.A. Alman, Phys. Scr. T 111 (2004) 145.
- [31] A. Kirschner et al., J. Nucl. Mater., these Proceedings. doi:10.1016/j.jnucmat.2004.10.104.
- [32] W. Jacob, J. Nucl. Mater., these Proceedings. doi:10.1016/j.jnucmat.2004.10.035.
- [33] M. Mayer et al., Mechanism of Hydrocarbon Layer Formation in Remote Areas of Fusion Devices, EPS, St. Petersburg, 2003.
- [34] G. Federici, J. Nucl. Mater., these Proceedings. doi:10.1016/j.jnucmat.2004.10.149.
- [35] G. Federici, ITER JWS Garching, 11th European Fusion Physics Workshop, (Heraklion 2003).
- [36] C. Brosset et al., J. Nucl. Mater., these Proceedings. doi:10.1016/j.jnucmat.2004.10.045.